Design considerations for linear Paul trap mass spectrometer under development

S.Sevugarajan and A.G.Menon
Department of Instrumentation,
Indian Institute of Science, Bangalore –560012, India.

Abstract

This brief note presents design considerations for a linear ion trap mass spectrometer in our laboratory. The motivation for this effort was to investigate the increased sensitivity that could be obtained in such a configuration in contrast to the conventional three-dimensional Paul trap mass analyzers. This technical report discusses the equation of ion motion and then the conditions for stability in the presence of a dc trapping field in the axial direction, we also present the influence of the trapping voltage, rod length and rf frequency on mass range.

Introduction

Linear quadrupole mass spectrometers [1,2] have been used for many years for the studying the spectroscopic and physical properties of ions [3,4]. The advantages of linear ion trap mass spectrometer include reduced space charge effect, increased ion trapping efficiency and increased ion storage volume [5] compared to the 3D Paul trap. Recently Schwartz et al. [6] have used resonance ejection in linear quadrupole mass spectrometer for enhancing the trapping efficiency compared to the conventional three-dimensional devices for the same operating parameters. Hager [7] utilized the coupling of radial and axial motion in the exit fringing fields in presence of an auxiliary quadrupole field for improving sensitivity. The following sections present the theory and the choice of choosing the rf frequency, rod length, trapping voltage for constructing a mass analyzer with high trapping efficiencies and high sensitivity.

Theory

The linear ion trap consists of a 4-rod assembly (similar to the quadrupole mass filter [1]) and two flat endcap electrodes. An rf potential, 180 degrees out of phase, is applied to pair of opposite electrodes for creating a linearly varying electric field in between the rod assembly. This electric field confines the ions in x and y direction. Two circular endcap electrodes kept at the ends of the four-rod structure with a small dc potential achieves confinement of ions in axial (z) direction. The two flat circular endcap electrodes also act as image current sensor for detecting the ion secular frequencies.

For obtaining a linear electric field inside a linear ion trap, the potential distribution should be quadratic [1]. Hence, we assume a quadratic potential distribution function with the magnitude ϕ_0 for confining the ions in x and y direction of motion which is given by

$$\phi_r = \frac{\phi_0}{2r_0^2}\left(a_1 x^2 + a_2 y^2 + a_3 z^2\right) \tag{1}$$

when there is an electric field it is necessary that it should satisfy the Laplace condition given by Eq. (2)

$$\nabla^2 \phi_r = 0 \tag{2}$$

Substituting Eq. (1) in Eq. (2) we get

$$\frac{\phi_0}{2r_0^2}\left(2a_1 x + 2a_2 y + 2a_3 z\right) = 0 \tag{3}$$

for Laplace condition to hold the bracketed term in Eq. (3) should be zero. Hence we have

$$\left(a_1 x + a_2 y + a_3 z\right) = 0 \tag{4}$$

since the linear ion trap is a two dimensional structure, $a_3 = 0$. If we let $a_1 = 1$ and $a_2 = -1$ for the Laplace condition to be satisfied, the potential function takes the form as given below.

$$\phi_r = \phi_0\left(\frac{x^2 - y^2}{2r_0^2}\right) \tag{5}$$

when a dc potential of magnitude U_0 and an rf potential of magnitude V_0 applied to the central four electrodes the magnitude of the potential ϕ_0 at any instant of time is given by

$$\phi_0 = \left(U_0 + V_0 \cos\Omega t\right) \tag{6}$$

Substituting Eq. (6) in Eq. (5) the potential function takes the following form.

$$\phi_r = \left(U_o + V_0 \cos\Omega t\right)\left(\frac{x^2 - y^2}{2r_0^2}\right) \tag{7}$$

The electric field created by the potential ϕ_r confines the ions in x and y direction. But the ions still have the freedom of moving in z-direction. In order to restrict the motion of ions

in z-direction, we apply a small static potential U_T to the endcap electrodes. Due to the geometry of the trap, the potential distribution ϕ_T inside the trap due to the potential U_T will be quadratic and hence it will have the following form.

$$\phi_T = \frac{\kappa U_T}{2d_0^2}\left(\alpha x^2 + \beta y^2 + \gamma z^2\right) \tag{8}$$

Where κ is the geometric factor that depends on the geometry of the linear ion trap and d_0 is half the magnitude of the rod length. Again for the Laplace condition to be satisfied the bracketed term in Eq. (8) should vanish. To achieve this we let $\alpha = 2$, $\beta = -1$ and $\gamma = -1$. After Substituting for the values of a, β and γ *in* Eq. (8) we have

$$\phi_T = \frac{\kappa U_T}{d_0^2}\left(z^2 - \frac{\left(x^2 + y^2\right)}{2}\right) \tag{9}$$

According to the superposition principle the effective potential inside the ion trap due to ϕ_r and ϕ_T is given by

$$\phi_{eff} = \phi_r + \phi_T \tag{10}$$

Substituting (7) and (9) in Eq. (10) we get

$$\phi_{eff} = \left(U_o + V_0 \cos\Omega t\right)\left(\frac{x^2 - y^2}{2r_0^2}\right) + \frac{\kappa U_T}{d_0^2}\left(z^2 - \frac{\left(x^2 + y^2\right)}{2}\right) \tag{11}$$

Simplifying Eq. (11) we get

$$\phi_{eff} = \left(U_0 - \Delta U_T + V_0 \cos\Omega t\right)\frac{x^2}{2r_0^2} - \left(U_o - \Delta U_T + V_0 \cos\Omega t\right)\frac{y^2}{2r_0^2} + \frac{\kappa U_T}{d_0^2} z^2 \tag{12}$$

where

$$\Delta = \frac{\kappa r_0^2}{d_0^2} \tag{13}$$

From classical mechanics, the equation of ion motion in x, y and z directions inside a linear ion trap having a potential distribution given by Eq. (12) and when there is no coupling between x, y and z direction of motions can be written as [9].

$$m\frac{d^2x}{dt^2} + e\nabla U_{eff}\left(x\right) = 0 \tag{14}$$

$$m\frac{d^2y}{dt^2} + e\nabla U_{eff}(y) = 0 \tag{15}$$

$$m\frac{d^2z}{dt^2} + e\nabla U_{eff}(z) = 0 \tag{16}$$

Substituting Eq. (12) in Eqs. (14), (15) and (16) and applying a transformation $\xi = \Omega t/2$ we have

$$\frac{d^2x}{d\xi^2} + \frac{4e}{mr_0^2\Omega^2}(U_0 - \Delta U_T + V_0\cos 2\xi)x = 0 \tag{17}$$

$$\frac{d^2y}{d\xi^2} + \frac{4e}{mr_0^2\Omega^2}(-U_0 - \Delta U_T - V_0\cos 2\xi)y = 0 \tag{18}$$

$$\frac{d^2z}{d\xi^2} + \frac{8eU_T}{md_0^2\Omega^2}z = 0 \tag{19}$$

Eqs. (17), (18) and (19) can be rewritten as

$$\frac{d^2x}{d\xi^2} + (a_x + 2q_x\cos 2\xi)x = 0 \tag{20}$$

$$\frac{d^2x}{d\xi^2} + (a_y + 2q_y\cos 2\xi)y = 0 \tag{21}$$

$$\frac{d^2z}{d\xi^2} + a_z z = 0 \tag{22}$$

where

$$a_x = \frac{4e(U_0 - \Delta U_T)}{mr_0^2\Omega^2} \tag{23}$$

$$a_y = -\frac{4e(U_0 + \Delta U_T)}{mr_0^2\Omega^2} \tag{24}$$

$$a_z = \frac{8\kappa e U_T}{m d_0^2 \Omega^2} \tag{25}$$

$$q_x = \frac{2eV_o}{m r_0^2 \Omega^2} \tag{26}$$

$$q_y = -\frac{2eV_o}{m r_0^2 \Omega^2} \tag{27}$$

when the dc potential applied to the central four rods (U_0) is assumed to be zero, the stability of the ions are determined by the trapping potential U_T and the rf potential V_0. The stability diagram in such case is shown in Fig. 1. As compared to the stability diagram in a Paul trap the linear ion trap does not have stable region in the positive a_u axis as the sign of a_u is negative (when $U_0 = 0$) in a linear ion trap where as it has both positive and negative values in a Paul trap. Similar result has been reported by Drewsen and Broner [8]. κ is purely an experimental parameter and its value is characterized by calibrating the mass spectrum for some known standard sample. For our computational purpose we have assumed it to have a value of 1.

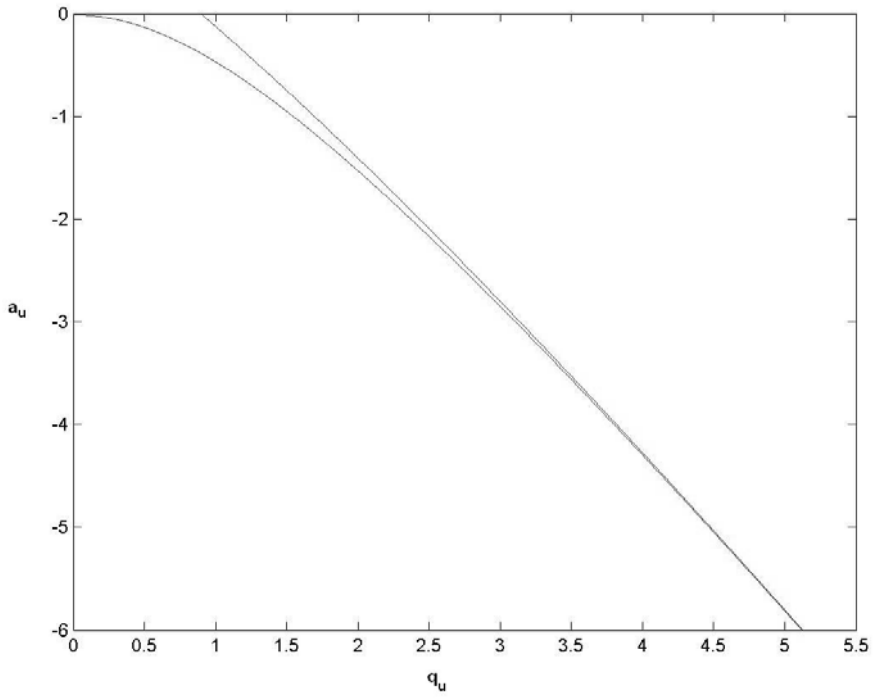

Fig. 1. Stability diagram of the linear ion trap under design

Unless and otherwise specified the following conditions are assumed for the following computations. Length of the four rods L_o = 7.5mm, inscribed field radius r_o = 3.5mm, magnitude of the rf potential is kept at $300V_{0\text{-}p}$ and the frequency of the rf potential Ω = 1MHz.

Secular frequencies (ω_u)

The characteristic frequency or the secular frequency of ion oscillation for a given experimental condition in x and y direction is determined by the Mathieu parameter β_u [1,2] which has a continuous fraction relationship [1,2] with a_u and q_u values given by Eq. (23), (24), (26) and (27). The secular frequency in the axial direction is determined by the second order linear differential equation given by Eq. (22) and is given by

$$\omega_z = \sqrt{a_z}\,\frac{\Omega}{2} \tag{28}$$

Trapping Voltage (U_T)

Fig. 2 shows the range of masses that can be stored in the trap for different trapping voltage U_T. The lower mass that can be trapped in the trap remains almost constant with 264 a.m.u for 1V and 261 a.m.u for 10V, where as the higher mass that can be trapped in the trap vary enormously depending on the magnitude of the trapping potential U_T applied to the endcap electrodes. From the Fig. 2, we can observe that the higher mass that can be trapped in a linear ion trap decreases proportionately with the increase in the trapping voltage.

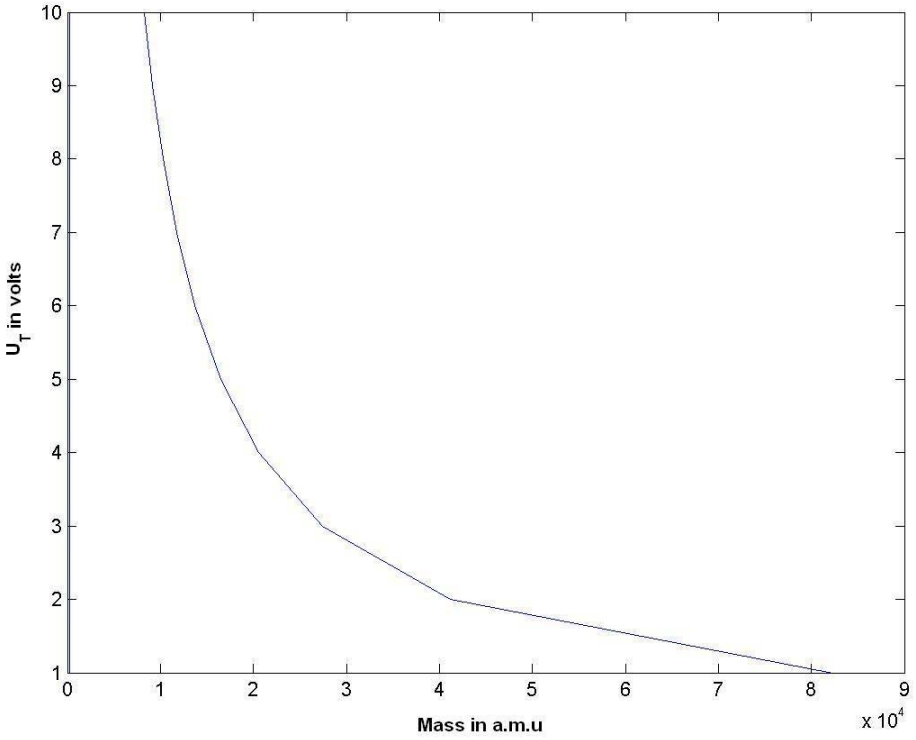

Fig. 2. Mass range for different trapping voltage U_T

Length of the trap (L_o)

The maximum mass that can be trapped in the trap for different values of L_o in terms of the inscribed field radius r_o is shown in Fig. 3. For plotting this figure the magnitude of the trapping potential U_T is fixed at 1V. It can be seen that the maximum mass that can be stored increases more than linearly as the magnitude of L_o/r_o increases. This shows that increasing the length of the trap electrodes can increase the mass range.

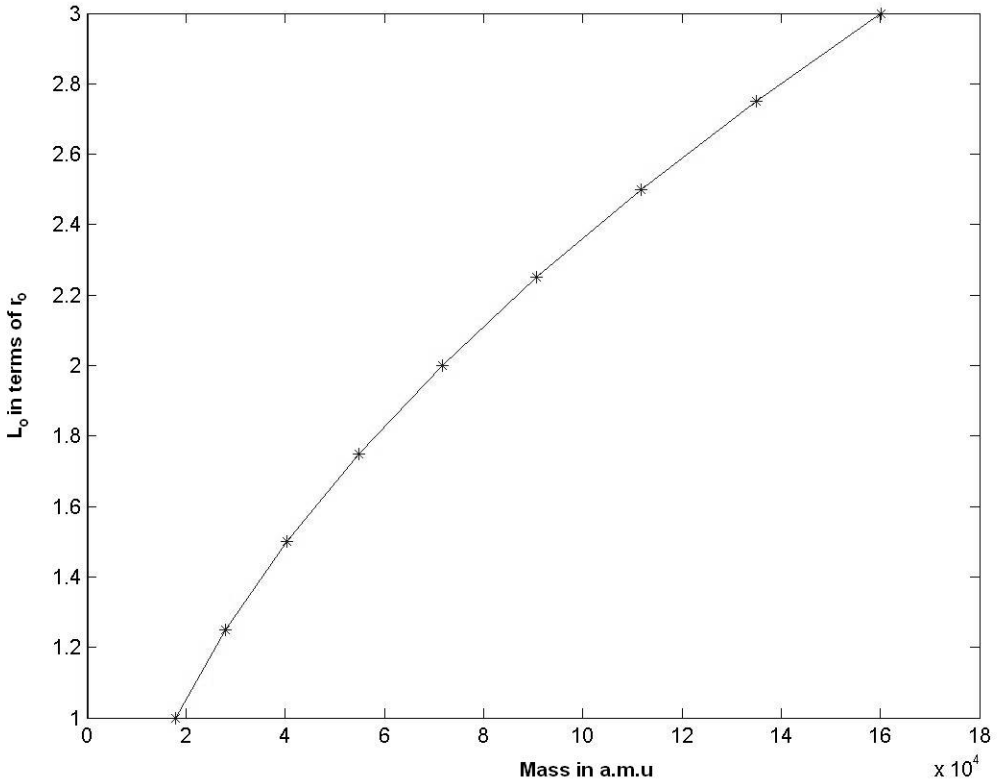

Fig. 3. Mass Range for different values of L_o expressed in terms r_o

rf drive frequency (Ω)

Fig. 4 and 5 shows the variation of lower and higher masses that can be trapped for different rf drive frequencies respectively. The magnitude of the trapping potential U_T is kept at 1V for computation purpose. Fig. 4 shows that increasing the rf drive frequency enables to trap much lower mass ions when compared to the higher rf drive frequencies, where as the maximum mass that can be trapped increases with the decrease in the rf drive frequencies as shown in Fig. 5.

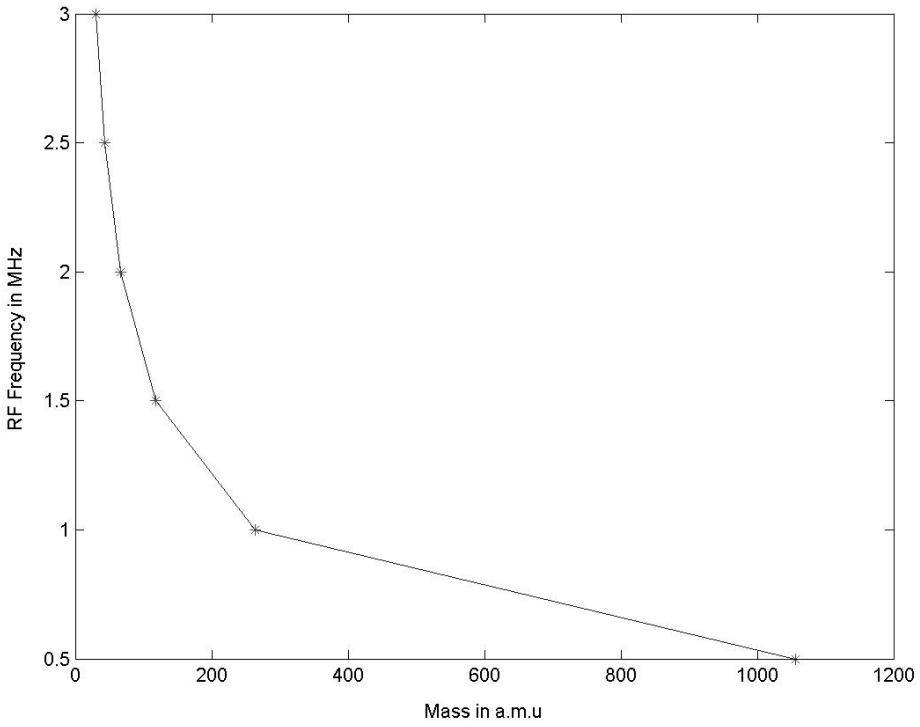

Fig. 4. Variation of lowest mass trapped for different rf drive frequencies

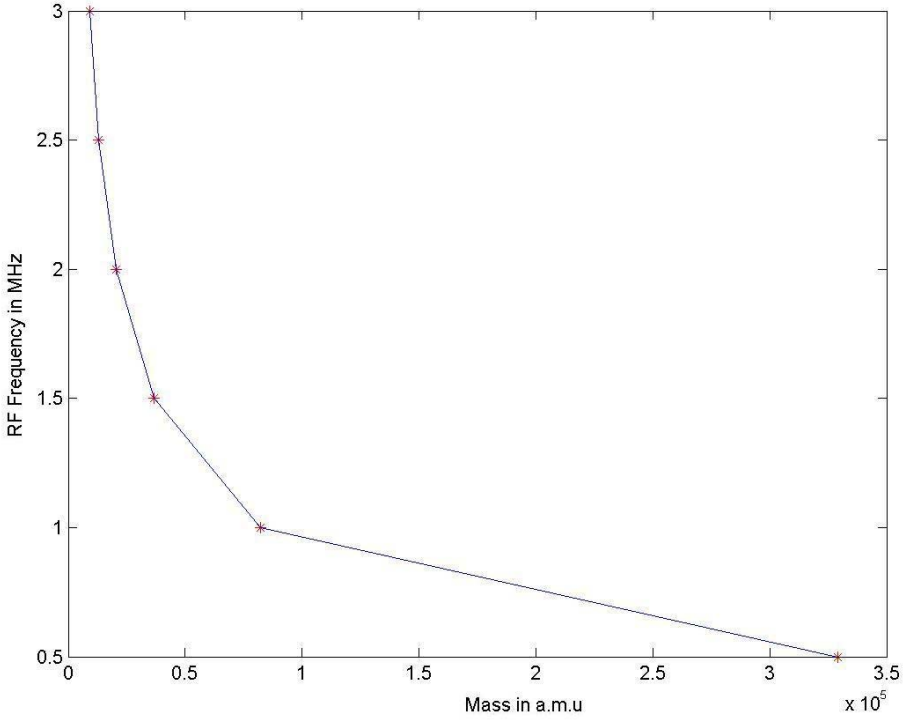

Fig. 5. Variation of highest mass trapped for different rf drive frequencies

Current Status

Mechanical design:

Fig. 6 and Fig.7, shows the zoomed portion of the linear trap and electron gun assembly. In our design we have kept the length of the four rods, L_o, as 15mm and the radius of the rods R_o as 3.5mm for achieving a field radius r_o of 3.05mm (please note, we have used 3.5mm as r_o in our computation) according to the relation $R_o = 1.148r_o$ given by Dawson [1] for circular rods. The endcap electrodes are spaced 1mm apart from the 4-rod assembly. One of the endcap has a 1mm diameter hole at the center for allowing the electrons for ionizing the sample gas. The ion gun assembly is mounted above this electrode. The ion gun consists of a tungsten filament, gating electrode and an extraction electrode. The gating electrode and the extraction electrodes are insulated with ceramic spacers. The linear ion trap along with the electron gun assembly is mounted on a CF100 flange with the help of two pillars as shown in Fig. 6. Feed throughs were inserted on the CF100 flange for electrical connection. The necessary vacuum is achieved by using a turbo molecular pump.

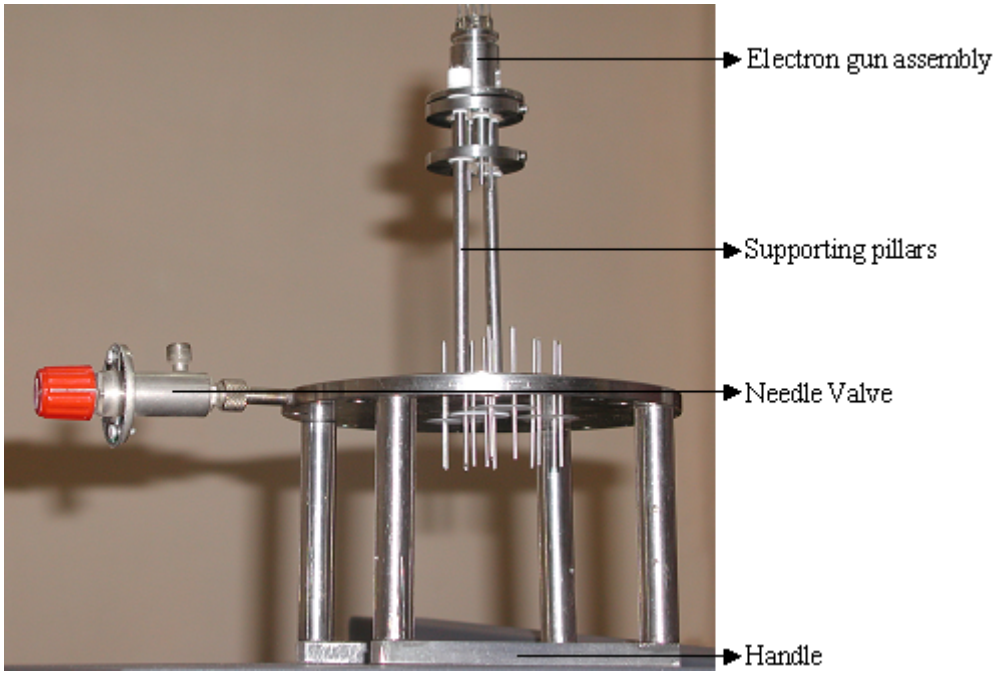

Fig. 6. Mechanical design of the Linear ion trap

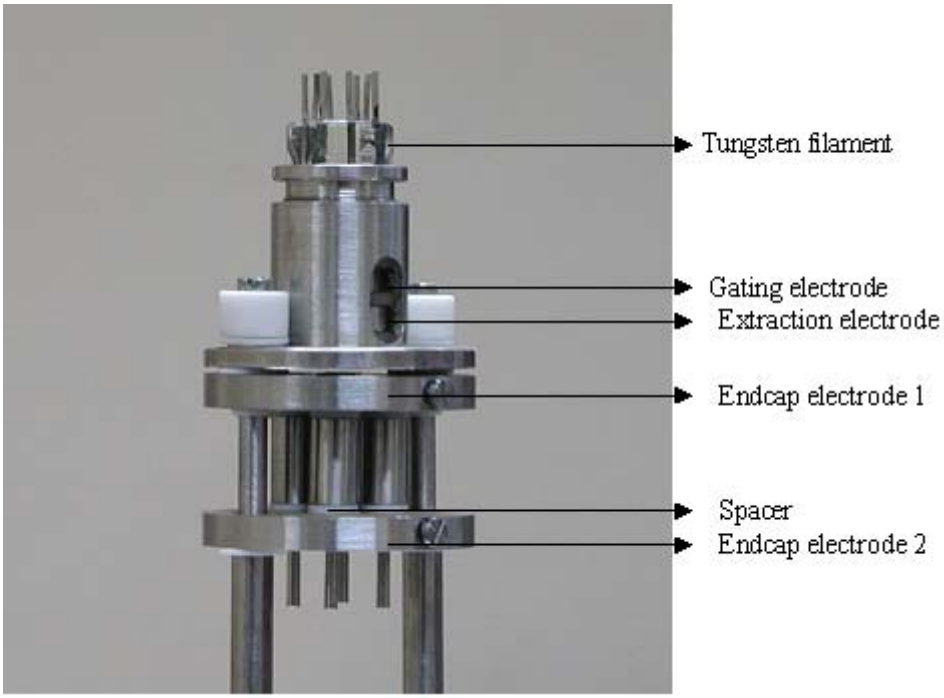

Fig. 7. Zoomed portion of electron gun and trap assembly

Vacuum System

The vacuum system consists of two ports, one compatible for CF100 flanges and the other one compatible for CF75 flanges. With this system design we can operate two mass spectrometers simultaneously for two different studies with the help of a single turbo molecular pump (our motivation was to connect our Paul trap to this vacuum system). BA gauge is used as a sensor for measuring the pressure inside the vacuum chamber. A rotary pump is used as a backing pump.

Electronics

Chassis housing all the electronic subsystems [10] required for the operation of the linear ion trap mass spectrometer except the rf power source is shown in Fig. 8. The rf power source has been isolated to avoid the interference of rf signal with other power supplies. This power supply unit has a 0-10amps constant current source for producing electrons from the tungsten filament by thermionic emission; a negative 0-150V voltage source for biasing the filament; two positive 0-150V voltage source one for the trapping potential, U_T, and the other for the extraction electrodes of the electron gun; and a ±150V voltage source for gating electrons into the trap. The rf power source [10] is designed to operate at a frequency of 4MHz and at $400V_{p\text{-}p}$. No dc potential will be applied to the rods. The power supplies required for the operation of the linear ion trap have been tested for their satisfactory performance on a Paul trap mass spectrometer in the laboratory.

The image current amplifier circuit for sensing the ion secular frequencies is currently under fabrication.

Fig. 8. Power supply unit for linear ion trap mass spectrometer

References

1. Dawson, P.H. Quadrupole Mass Spectrometry and its Application, Elsevier, Amsterdam, 1976.

2. March, R.E. and Hughes, R.J. Quadrupole Storage Mass Spectrometry, Wiley-Interscience Publications, New York, 1989.

3. Prestage, J. D., Dick, G. J. and Maleki, L., J. Appl. Phys., 66 (1989) 1013-1017.

4. Birkl, G. and Kassner, S., Nature, 357 (1992) 310-313.

5. Syka, J. E. P and Fies, W. J. Jr. Fourier Transform Quadrupole mass spectrometer and method, US Patent, 4755670, 1988.

6. Schwartz, J. C., Senko, M. W. and Syka, J. E. P., J. Am. Soc. Mass Spectrom., 13 (2002) 659-669.

7. Hager, J. W., Rapid Commun. Mass Spectrom. 16 (2002) 512-526.

8. Drewsen, M. and Broner, A., Phy. Rev. A, 62 (2000) 045401-1 to 045401-4.

9. Landau, L.D. and Lifshitz, E.M. Mechanics, Third Edition, Pergamon, UK, 1976.

10. Paul, J., Linear Ion Trap Mass Spectrometer Instrumentation, Unpublished M.Tech Project Report, Department of Instrumentation, Indian Institute of Science, Bangalore, India, Jan (2003).